PAPER

Joint Description Methods of Wind and Waves for the Design of Offshore Wind Turbines

AUTHOR

Kim E. Mittendorf

Vestas Technology R&D Americas, Inc.

ABSTRACT

Wind and wave loads are equally important for the design of offshore wind energy structures. For the design against an ultimate limit state or fatigue, the engineer has to estimate the combination of loads that are likely to occur simultaneously during the design life of the wind turbine. This is quite a complex task, involving different wind/wave models, load-calculation methods and statistical analysis of simultaneous extreme wind and wave conditions. Moreover, reliable and realistic methods for the assessment of the service life of an offshore wind energy converter under combined wind and wave loads are necessary. However, the current design guidelines (Det Norske Veritas or German Lloyd) provide hardly any information on how to model the wind and wave correlation. In this article, several approaches for obtaining the required wind-wave correlation for the design have been investigated. Manual wave forecasting methods, spectral sea state descriptions and numerical wave model data have been compared to simultaneously measured wind and wave data from the FINO research platform in the German Bight of the North Sea. The used approaches are general and can be easily applied to different data sets from different regions.

Keywords: wind-wave correlation, offshore wind energy, joint probability, design, loads

Introduction

To make offshore wind energy economically viable, it is necessary to develop concepts for highly optimized and robust Offshore Wind Energy Converters (OWEC) with a long life span. The move from land to sea requires a change in the design of wind energy converters. Therefore, existing design methods have to be improved or even new ones have to be developed, which, in addition to the standard loads, take wave loads into account.

During the design process, the engineer has to estimate the worst as well as the fatigue loading condition a wind energy turbine is likely to be exposed to during its lifetime. This is quite a complex task, involving different wind/wave models, load-calculation methods and extreme event analyses.

For a simulation of an OWEC in the time domain, the water surface displacements (i.e., the waves) and the variation of the wind velocities have to be realistically generated. The resulting loads are quite sensitive to the chosen correlation model for wind and waves.

In this paper, the following methods for determining sea state characteristics for a certain wind will be applied and compared with each other, as well as with measured field data:

- Statistical correlation methods with jointly measured wind and wave data
- Wave forecasting methods
- Numerical sea state hindcast (covering a 12-year period)
- Joint probability modeling

The combined measured wind and wave data sets are taken from the research platform Forschung in Nord-Ostsee (FINO). The platform is located in the German Bight at N54°0.86’ E6° 35.26’, about 45 km north of the Island of Borkum in the North Sea (Figure 1) (http://www.fino-offshore.de; Neumann et al., 2004).

Analysis of Jointly Measured Wind and Wave Data

The instantaneous values of water surface displacement and wind speed can be regarded as uncorrelated. However, there exists some correlation between the mean wind speed and significant wave height. In Figure 2, the significant wave height H_s is plotted against the 10-min mean wind speed at 100-m height. The wind speed has been taken exactly at the same time (red triangle), 1 h before (blue circle) and 1 h after (green cross) the significant wave heights have been measured. No major differences are observed in the scatter plots of the data. Thus, only wind and wave data measured in the same time interval are regarded in the further analysis. Best fit lines are shown in Figure 4.

The following measured data are used in the analysis:

Wind	
Considered period	November 2003 to May 2005
Data type	10-min mean values of the wind speed at 100-m height
Data coverage	87,401 data sets are measured, which correspond to a coverage of 95% of the considered time period
Mean	10.0584 m/s and variance: 23.25 m^2/s^2

The cumulative distribution function of the 10-min mean wind speed U_{m100} at 100-m elevation is interpreted from the wind measurement alone and is fitted to a 2-parameter Weibull distribution (a = 11.3574 and c = 2.20229). A visual inspection of the data plot in Weibull scale indicates that the data fall on a straight line.

Waves	
Period	November 2003 to May 2005
Data type	1-h significant wave height H_s from wave buoy
Data coverage	10,024 data sets are measured, which correspond to a coverage of 65.367% of the considered time period
Mean	1.4816 m and variance: 0.92335 m^2

The cumulative distribution function of the significant wave height H_s is interpreted from the buoy measurement and is fitted to a Weibull function (with parameters a = 1.66648 and c = 1.65229) as well. The significant wave height data plotted on Weibull probability paper almost fall on a straight line. Deviations from the straight line in the far upper tail may be ascribed to statistical uncertainty among the few largest observed significant wave heights and possibly also to a few of the readings belonging to the same extreme storm and thus being highly correlated.

Correlation of Measured Wind and Wave Data

If no simultaneous wind and wave measurements are available, the simplest approach to correlate mean wind speeds and significant wave heights is to assign values with equal cumulative probabilities. In the case of wind and wave data

$$CDF_{Wind} = CDF_{Waves}$$

CDF is the cumulative distribution function.

The relationship between the mean wind velocities U_{m100} and significant wave height H_s with equal probability is shown in Figure 3. The data of H_s (U_m) are fitted to 4th degree polynomial:

$$H_s(U_m) = p_1U_m^4 + p_2U_m^3 + p_3U_m^2 + p_4U_m + p_5$$

with $p_1 = 7.741 \times 10^{-7}$, $p_2 = -8.736 \times 10^{-5}$, $p_3 = 0.005328$, $p_4 = 0.1038$, $p_5 = -0.08235$.

FIGURE 1

Location of FINO platform (BSH, 2002) and sketch of structure (FINO-OFFSHORE, 2004).

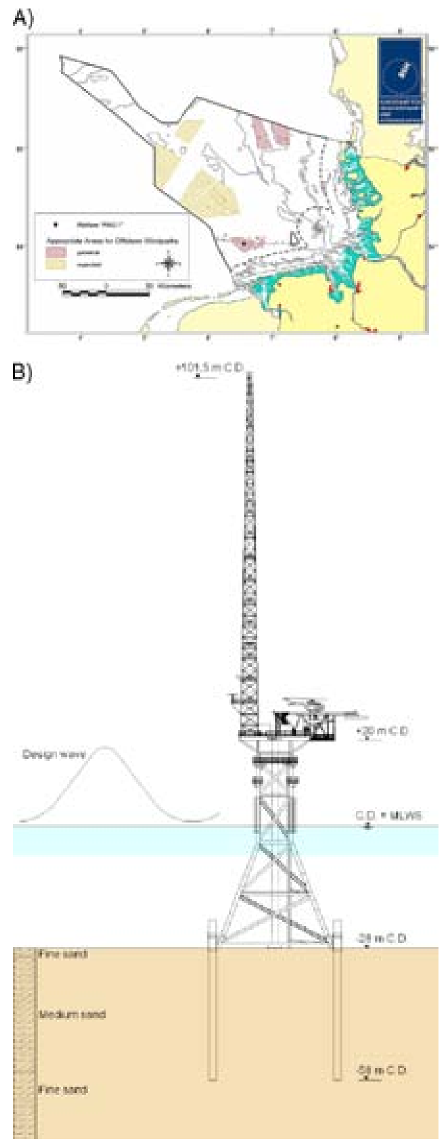

The FINO data consist of pairs of measured wave height and wind speed (H_s, U_{m100}), which allows to directly derive a joint description of the data. For a given mean wind speed, models for expected H_s are calibrated to the data:

- Model 1: Cubic polynomial fit

$$H_s(U_m) = p_1U_m^3 + p_2U_m^2 + p_3U_m + p_4$$

with $p_1 = -3.046 \times 10^{-6}$, $p_2 = 0.005447$, $p_3 = 0.008356$, $p_4 = 0.7137$.

FIGURE 2

Scatter plot of significant wave height against 10-min mean wind speed at 100-m elevation (FINO 2003-2005).

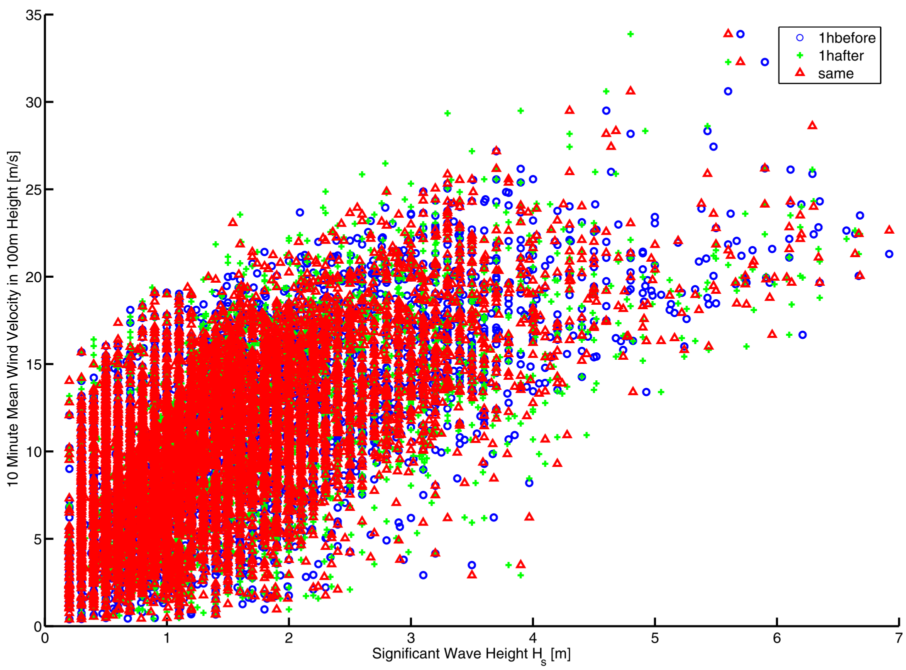

- Model 2: Exponential fit type 1

$$H_s(U_m) = a \times \exp(b \times U_m)$$

with a = 0.6165 and b = 0.079.

- Model 3: Exponential fit type 2

$$H_s(U_m) = a \times \exp(b \times U_m) + c$$

with a = 0.8311, b = 0.06867 and c = −0.2876.

In Figure 4, the measured mean wind speed is plotted against the significant wave height. In general, the data have a distinctive variability.

The fitted model results are also included in the plot and are apparently in good agreement with the observations. Above a wind speed of 25 m/s, the deviations appearing between the measurement and model get larger, which is mainly caused by limited amount of data in the high wind regime. For higher wind velocities, the data are not only rare, but they also show a large scatter.

In the far upper tail, the chosen models therefore have larger deviations. The smallest root mean square error (RMSE) between the measured data and model is smallest for the cubic polynomial fit with RMSE = 0.6908. So, it is concluded that the cubic polynomial fit gives the best results for the measured wind and wave data.

In comparison, method 1 ($CDF_{Wind} = CDF_{Waves}$), where values of equal probabilities have been used, gives slightly higher mean significant wave heights for a given mean wind velocity in the range of 5 m/s up to 25 m/s than method 2, which tries to find the best curve fit. In the upper tail, the deviation between methods 1 and 2 decreases. The standard deviation of the residuals of the difference between methods 1 and 2 is s = 0.38174.

Both methods do not take into account the observed scattering in the data. The models are only fitted to average values. A more detailed view with less scatter may be obtained from an analysis of the wind and wave data with respect to certain direction sectors and single storm events. Another reason for the variability of the wind and wave data is that the fetch length as well as the duration of the wind blowing is not considered in the analysis. Nevertheless, these results lead to the conclusion that method 1 can be applied for predicting mean values if no combined

FIGURE 3

Wave height vs. mean wind velocity with equal probability (FINO).

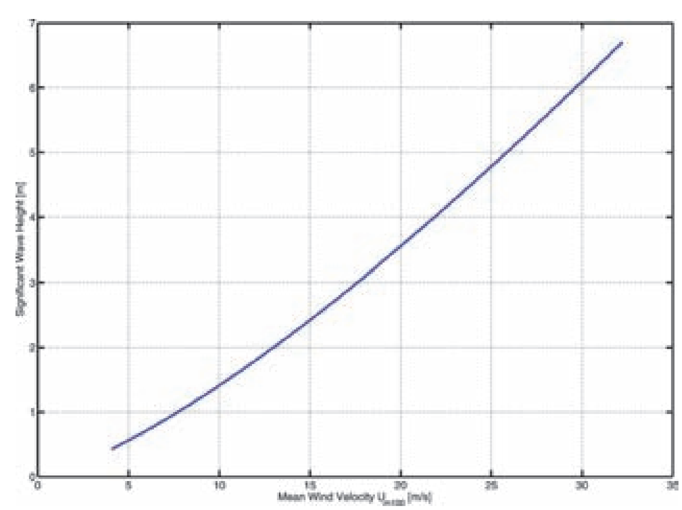

FIGURE 4

Comparison of wind and wave correlation methods (FINO).

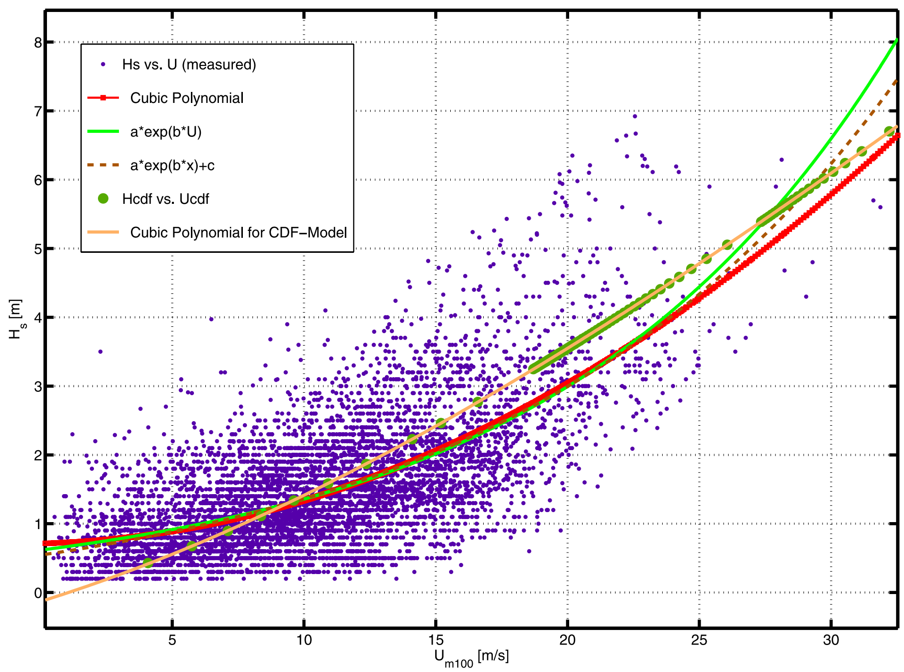

wind and wave measurements are available, but results for higher wind or wave values should be used with care.

Manual Wave Forecasting Methods and Spectral Sea State Description Model

In literature, many empirical formulas describing the significant wave height from known properties of the wind field can be found. They are based on ship observations and/or site measurements. The existing formulas have a limited application range because of their inherent assumptions and simplifications. However, their simplicity makes them very attractive for engineering applications.

Sverdrup and Munk (1947) and Bretschneider (1952) have been among the first who attempted to predict fetch-limited wave heights. They related the wave energy and frequency to the fetch, and the non-dimensional growth curves became known as the Sverdrup Munk Bretschneider (SMB) curves.

The formulation by Neumann and Pierson (1966) is valid only for fully developed wind waves in deep water. It relates the mean wind speed U_m to the significant wave height H_s and mean wave period T_z:

$$\begin{aligned} H_s &= \frac{0.21}{g}U^2 \\ T_z &= 0.81\left(\frac{2\pi}{g}U\right) \end{aligned} \tag{1}$$

When the fetch becomes very large, the wave growth will cease and is called fully developed. For fully developed sea state, Pierson and Moskowitz (1964) gave a spectral description $S_{pm}(\omega)$, in which significant wave height and mean wind speed have been used.

The significant wave height H_s is the 0th moment of the spectrum, defined as

$$H_s = 4\cdot\sqrt{\int S(\omega)\omega^0 d\omega} \tag{2}$$

Thus, it is also possible to derive a relationship between the mean wind and the significant wave height. The PM spectrum $S(\omega)$ considers the wind speed as an input parameter to predict the wave energy.

Another approach to describe the fetch–limited wave evolution has been undertaken by Hasselmann et al. (1973) in the "Joint North Sea Wave Project (JONSWAP)". The relationship between wave energy, wind speed, fetch length and duration is given in spectral form, the JONSWAP spectrum $S_{js}(\omega)$.

The TMA spectrum $S_{tma}(\omega)$ is a modified JONSWAP spectrum where the JONSWAP spectrum is multiplied by a function that is depth and frequency dependent (see Bouws et al., 1985). This formulation relates the mean wind speed and significant wave height in regions with limited water depth, and it takes into account the shallow water effects, such as shoaling and wave breaking.

The above formulations are applied to the measured wind speeds from the FINO platform. The maximum possible fetch lengths for the FINO are estimated and are summarized in Table 1.

Figure 5 shows the significant wave height H_s as a function of the mean wind speed U_{10} in 10-m height derived from wave growth relationships.

The Pierson-Moskowitz spectrum describes a fully developed sea state, the JONSWAP spectrum and fetch-limited seas, and the TMA spectrum represents fetch-limited seas in intermediate water depth (d = 33.7 m).

TABLE 1

Estimated fetch lengths for FINO location.

Directional Sector	Distance
N	500 km
NWW	1500 km
NW	850 km
W	450 km
SW	500 km
S	50 km
SE	100 km
E	100 km
NE	150 km

The cross markers represent the measured data from the FINO platform. The curves represent an upper and lower boundary for the wave heights resulting from the fetch lengths given in Table 1. The main wind directions during the observation period (December 2003 to May 2005) are in the range of south (180°) to west (270°). The maximum possible fetch lengths X in this directional sector varies between 50 km and 550 km, which are chosen here as the upper and lower limits for the TMA and JONSWAP spectra.

The Pierson-Moskowitz formulation has no upper bounds and overestimates the wave heights for higher wind speeds. In general, the JONSWAP prediction gives a better fit. For the longest fetch distance, the wave heights are overestimated. An analysis of the distribution of the mean wind direction indicates that most of the time, the wind comes from south-west. This seems to justify the choice of the maximum fetch length of 500 km in the investigation. Moreover, this presumption is supported by the application of the TMA-spectrum, which gives a better representation of the measured data. The TMA-spectrum considers water depth effects, and the comparisons of the model results and measured data lead to the conclusion that these effects are important for the FINO location. The limitation of the maximum significant wave heights is justified too.

If the input data are ordered by fetch lengths, fetch duration, wind direction, fully developed sea state or developing sea state, then the fit between measured data and empirical formulas can be improved. This approach will get rather complex and will lose its simple applicability. Often, the available data will not contain all information needed. The fetch duration and length are rather difficult to evaluate.

For the storm event recorded during December 12 and 17, 2003, the manual forecast methods are compared with measured data and their derived relationship. The main wind direction was north-west. The measured data are best represented by the TMA spectrum. The correlation method 1 ($CDF_{Wind} = CDF_{Waves}$) and the fit of the complete data set (method 2) give an underestimation of the observed significant wave heights. In contrast to this, the JONSWAP spectrum overestimates the wave heights.

FIGURE 5

Significant wave height as a function of mean wind speed (TMA, JONSWAP, PM).

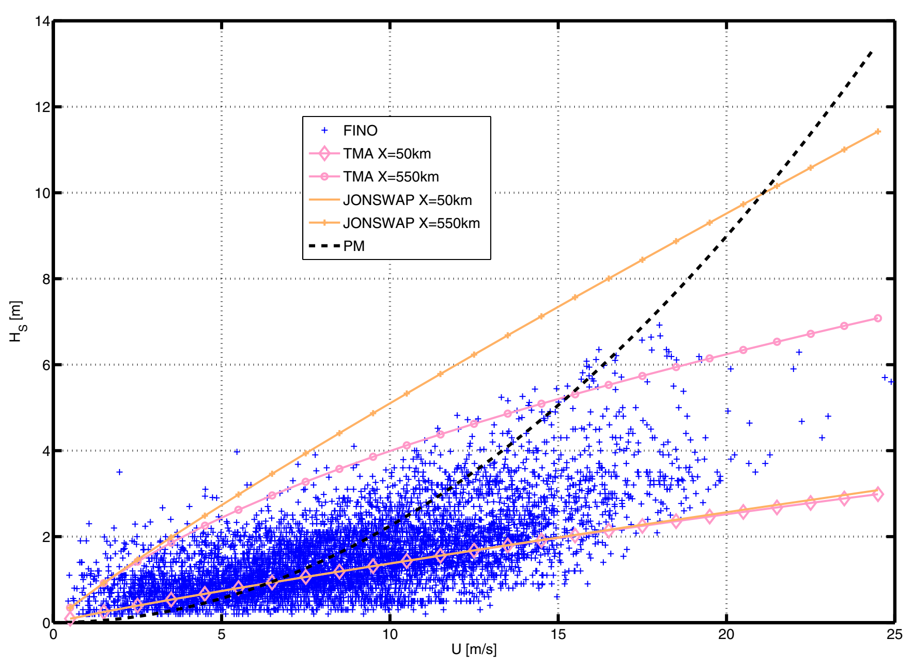

Numerical Wave Hindcast for the FINO Location

The results of the numerical hindcast model for the German Bight, which are described by Mittendorf and Zielke (2004) and Mittendorf (2006), are investigated with regard to the wind and wave correlation. The hindcast data cover the period from January 1989 to December 2000. The mean wind speed and the significant wave height are available every 3 h during this period.

The scatter plot of wind and wave data of the numerical hindcast is rather similar to the FINO data. Both data sets are fitted to a polynomial given by

$$f(x) = p_1 \times x^3 \times p_2 \times x^2 + p_3 \times x + p_4 \quad (3)$$

with corresponding parameters given in Table 2. The raw data and fitted polynomials are shown in Figure 6. The curve fitting leads to the conclusion that the hindcast overestimates the significant wave heights for higher wind speed.

Joint Probability Model for Mean Wind Speed and Significant Wave Data

This section presents an approach for the derivation of design conditions from simultaneously measured wind and wave data, including the variability within the data.

The wind loads and the wave loads originate from two concurrent load processes based on the characteristic design parameters. As it has been shown in the previous sections, the resulting parameters are quite sensitive to the correlation model chosen for wind and waves.

In this approach, the design parameters are specified by a mean wind speed, significant wave height and wave period. Used wave climate variables are the 3-h-significant wave height H_s and the mean zero-crossing period T_z. The used wind climate variable is the 10-min mean wind speed U_{10}.

A simultaneous description of wind and waves is given by a joint density distribution of the characteristic parameters. For the representation of concurrent waves and wind, it is feasible to model one climate variable as independent and the other climate variable as dependent. If the climate parameters are represented by continuous distribution functions, the following statistical procedure can be used to develop a joint probability density.

FIGURE 6

Distribution of significant wave and mean wind data (FINO Measurement and Hindcast).

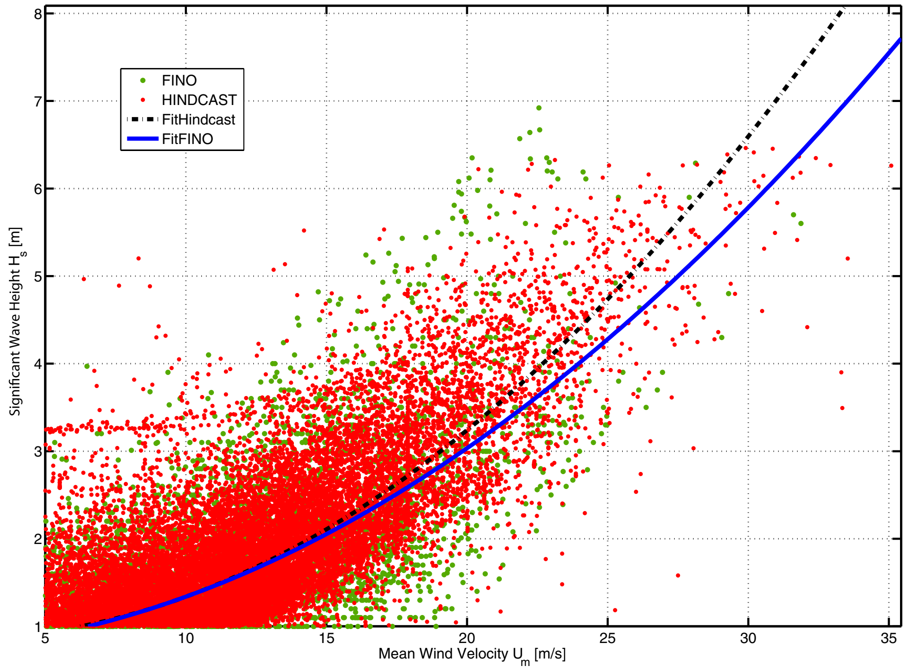

The joint density distribution of the characteristic parameters mean wind speed U_{10}, significant wave height H_s and mean wave period T_z is expressed as follows (Meling et al., 2000):

$$f(U_{10}, H_s, T_z) = f(U_{10}) \times f(H_s|U_{10}) \times f(T|H_s U_{10}) \quad (4)$$

where $f(U_{10})$ is the marginal distribution of U_{10}, $f(H_s|U_{10})$ is the conditional distribution of H_s for given U_{10} and $f(T|H_s\ U_{10})$ is the conditional distribution of T_z given H_s and U_{10}.

Marginal Distribution for the Mean Wind Speed

The marginal distribution $f(U_{10})$ is obtained by fitting all 10-min mean wind speed data to a two-parameter Weibull distribution. Based on FINO measurement for the time period from November 2003 to May 2005, the Weibull shape c and scale parameter a are determined (a = 11.789 and c = 2.310).

$$F(U_{10}) = 1 - \exp\left(-\left(\frac{U_{10}}{a}\right)^c\right) \quad (5)$$

where c is the shape parameter and a is the scale parameter.

TABLE 2

Fitted polynomial parameters.

Data Set	p_1	p_2	p_3	p_4
Numerical hindcast	0.00726	−0.0276	0.8885	0.0
FINO measured	-3.046×10^{-6}	0.005447	0.008356	0.7137

FIGURE 7

Density function for significant wave heights for every mean wind speed class (10-18).

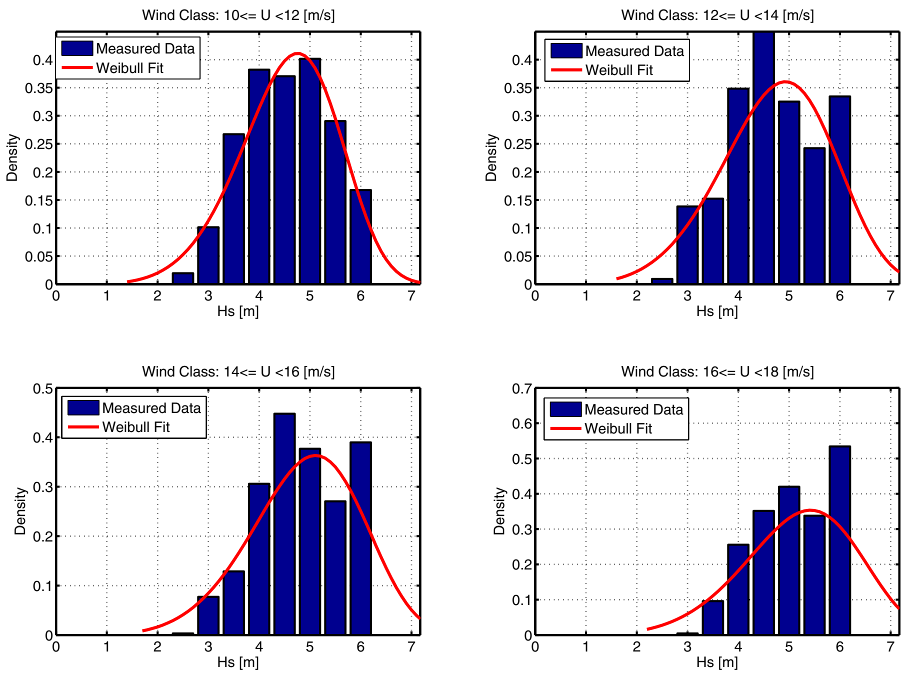

Conditional Distribution of Significant Wave Heights

In the next step, the wind data are divided into classes of 2 m/s of mean wind speed, and the corresponding wave heights to every wind speed class are also fitted to Weibull distributions. An example is given in Figure 7.

The graphs indicate that the adapted probability distributions give a satisfactory fit. The resulting Weibull parameters of the wave heights are expressed as a function of the wind speed, thus a continuous description of the conditional distribution of H_s is obtained.

The scale parameter a is parameterized as

$$a_{fit} = p_1 + p_2 \times U_{10}^{p3} \tag{6}$$

with p_1 = 0.7704, p_2 = 0.01304 and p_3 = 1.7696.

The RMSE of the fitted curve to the discrete point is 0.1247. Figure 8 shows the fitted Weibull parameters against the Weibull parameters of the measured data.

The shape parameter c is parameterized as

$$c_{fit} = r_1 + r_2 \times U_{10} \tag{7}$$

with r_1 = 1.535 and r_2 = 0.01304.

The RMSE of the fitted curve to the discrete point is 0.2116. Figure 9 shows the fitted Weibull parameters against the Weibull parameters of the measured data.

Furthermore, the two parameters a_{fit} and c_{fit} will be used to determine

FIGURE 8

Scale parameter estimated from the measurements vs. curve fit.

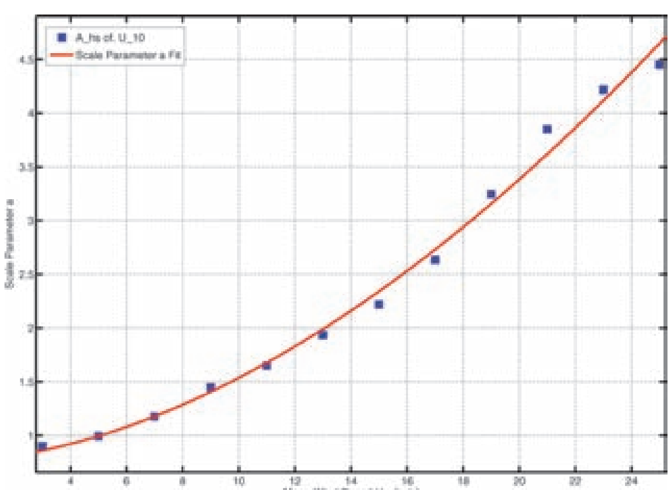

FIGURE 9

Shape parameter estimated from the measurements vs. linear fit.

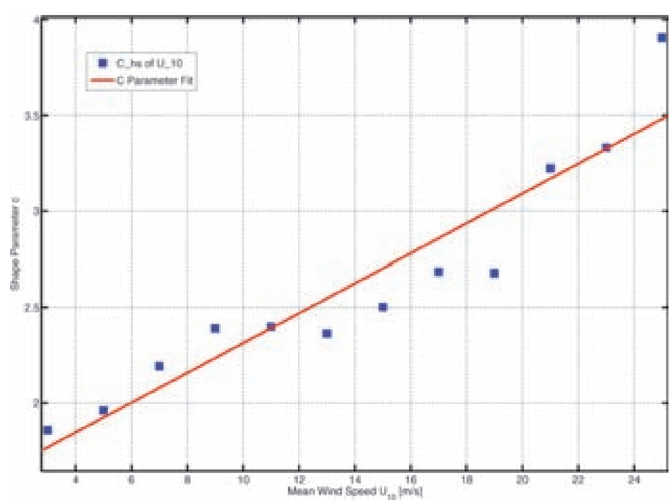

FIGURE 10

Expectation value of significant wave height given the mean wind speed.

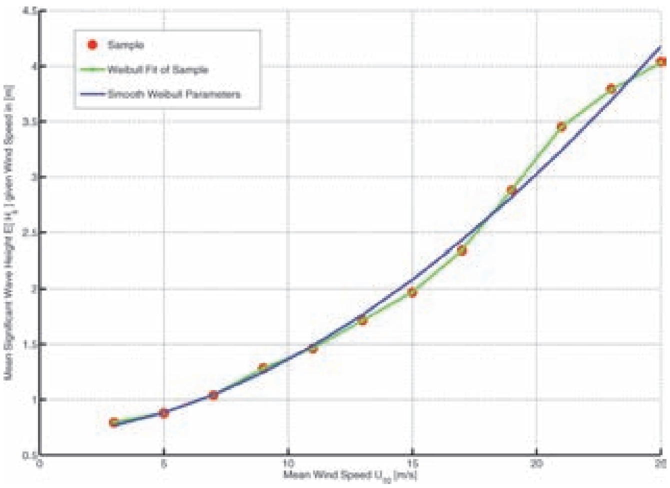

FIGURE 11

Standard deviation of significant wave height given the mean wind speed.

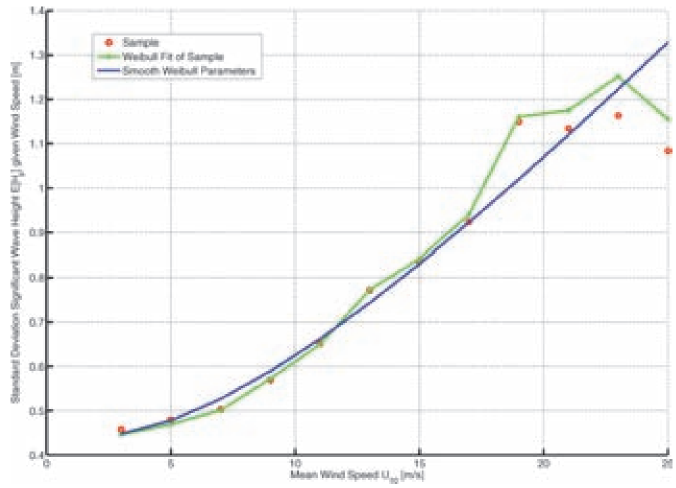

the conditional mean and mode values and standard deviation of the significant wave height given the mean wind speed. The sample values, the fitted Weibull and the smooth Weibull results for mean, mode and standard deviations are plotted in Figure 10, 11, and 12.

$$
\begin{aligned}
E[H_s] &= a_{fit} \times \Gamma\left(\frac{1}{c_{fit}} + 1\right) \\
STD[H_s] &= a_{fit} \times \left[\Gamma\left(\frac{2}{c_{fit}} + 1\right) - \Gamma\left(\frac{1}{c_{fit}} + 1\right)\right]^{0.5} \\
Mode[H_s] &= a_{fit} \times \left[1 - \frac{1}{c_{fit}}\right]^{1/c_{fit}}
\end{aligned}
\tag{8}
$$

Conditional Distribution of Mean Wave Periods for Given Wave Heights and Mean Wind Speeds

The mean wind velocities are sorted into classes with a bin size of 2 m/s in the range of 2 to 26 m/s, which gives 12 classes. Above 26 m/s, only 16 measured values are available. In every mean wind speed class, the significant wave heights are sorted into wave classes with a bin size of 0.5 m in the range of 0.25 m to 6.25 m, giving 12 classes too. All together, this gives 144 combinations of wind velocities and wave heights.

Consequently, the amount of data for every combination is rather limited, which gives higher uncertainty in the estimates and also complicates the process of finding a suitable distribution function for the mean crossing wave period T_z for the given significant wave height and mean wind speed.

The plots of the distribution of T_z in all wind-wave classes indicate that a log-normal distribution will be suitable despite limited amount of data and partly non-smooth histogram plots.

$$
f(T_z|H_s, U_{10}) = \frac{1}{T_z \times \sigma_{\ln(T_z)}\sqrt{2\pi}} \times \exp\left(\frac{1}{2}\left[\frac{\ln(T_z) - \mu_{\ln(T_z)}}{\sigma_{\ln(T_z)}}\right]^2\right) \tag{9}
$$

where $\sigma_{\ln(T_z)}$ is the standard deviation of $\ln(T_z)$ and $\mu_{\ln(T_z)}$ is the expectation value of $\ln(T_z)$.

The mean value and the standard deviation of T_z are calculated for every combination of H_s and U_{10}. These values are needed for the determination of standard deviation $\sigma_{\ln(Tz)}$ and expectation value $\mu_{\ln(Tz)}$ of the log-normal distribution of $\ln(T_z)$.

$$
\begin{aligned}
\mu_{\ln(T_z)} &= \ln\left[\frac{\mu_{T_z}}{\sqrt{1+\nu_{T_z}^2}}\right] \\
\sigma_{\ln(T_z)} &= \ln\left[\nu_{T_z}^2 + 1\right] \\
\nu_{T_z} &= \frac{\sigma_{T_z}}{\mu_{T_z}}
\end{aligned}
\tag{10}
$$

where σ_{T_z} is the standard deviation of T_z from measurement and μ_{T_z} is the mean value of T_z from measurement.

A visual inspection of the 3-D surface plot of the expectation value of the mean wave period T_z as a function of H_s and U_{10} reveals that, for a constant wave height H_s, the mean wave period $E[T_z]$ decreases with increasing mean wind speed U_{10}. For a constant wind speed U_{10}, the periods $E[T_z]$ increase with increasing wave heights.

This behavior can be described with the following function (Meling et al., 2000):

$$
\overline{T}(U_{10}, H_s)_z = \overline{T}_z(H_s) \times \left[1 + \theta\left(\frac{U_{10} - \overline{U}_{10}(H_s)}{\overline{U}_{10}(H_s)}\right)\right] \tag{11}
$$

where $T_z(H_s)$ is the conditional expectation value of the mean wave period given the significant wave height, $U_{10}(H_s)$ is the conditional mean wind speed given the significant wave height and $\theta = 0.67$ is the variation coefficient for $E[T_z]$ with wind speed given the wave height.

The conditional expectation value of the mean wave period T_z for a given wave height is parameterized in the following manner (Figure 13):

$$
\overline{T}_z(H_s) = p_1 + p_2 \times H_s^{p_3} \tag{12}
$$

with $p_1 = 3.513$, $p_2 = 1.245$ and $p_3 = 0.8035$.

FIGURE 12

Mode value of significant wave height given the mean wind speed.

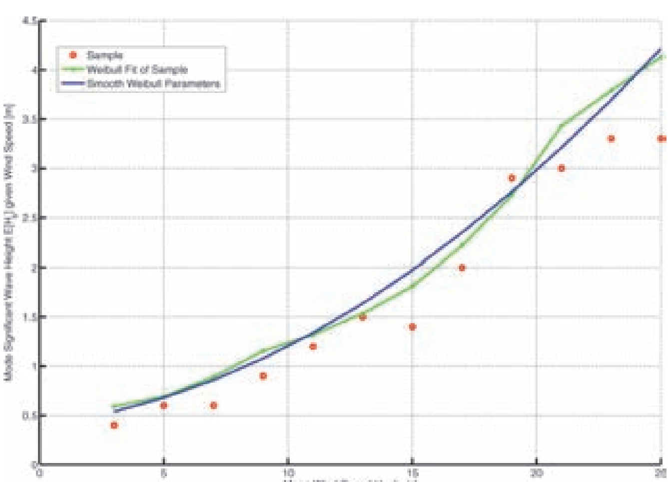

FIGURE 13

Conditional expectation value of the mean wave period given the significant wave height.

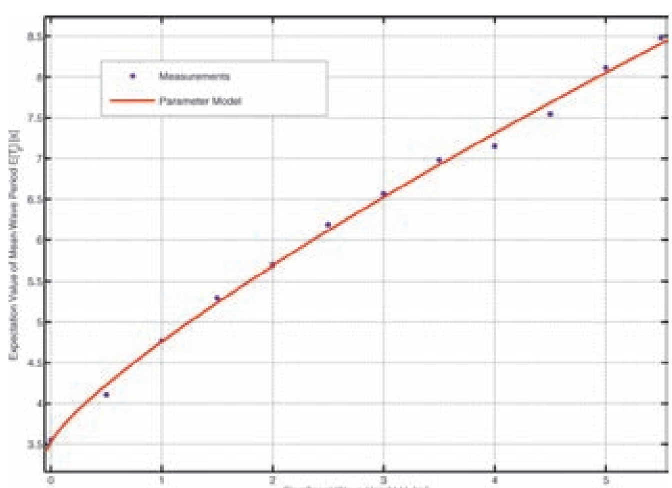

Correspondingly, the parameterization of the mean wind speed (Figure 14) is chosen to be

$$\overline{U}_{10}(H_s) = p_1 + p_2 \times H_s^{p_3} \tag{13}$$

with p_1 = 8.798 , p_2 = 0.004035 and p_3 = 3.781.

Absolute differences of model and measured mean periods serve to evaluate the goodness of the model. On average, the predicted wave periods deviate about 0.43 s from the measured data.

Finally, the joint distribution for mean wind speeds significant wave heights can be expressed by inserting the parameters above in the joint density distribution equation. The joint environmental model of mean wind significant wave heights and mean wave periods allows a simultaneous description of all considered sea state parameters, including their distribution. The model is expected to be of reasonable accuracy, but this accuracy depends strongly on the measured data base.

One disadvantage of this model approach is the demand on synchronous wind and wave data. For a reliable long-term prediction, longer data series would be required.

Furthermore, this model can be used for long-term predictions on the basis of contour line approaches by Winterstein et al. (1993) for different combinations of mean wind speed and significant wave height. Therefore, the subsequent joint probability density $f(U_{10}, H_s, T_z)$ of the parameters is transformed into a non-physical space consisting of uncorrelated standard Gaussian variables. In this space, the 50- or 100-year combinations will be located on a sphere with a radius r. To get the results in the physical space, a back transformation is necessary. Each contour for an associated return period describes an infinite number of combinations between U_{10}, H_s and T_z.

Conclusions

A straight forward application of the manual wave forecast methods gives rather good results for the wave height prediction. If all unsorted wind data are taken into account, only the average wind-wave behavior would be represented. A separate approach for all single storm events or events with the same wind direction and/or fetch length and duration improves the predictions but suffers from the fact that the simple applicability of this approach is lost.

The correlation methods based upon equal probabilities ($CDF_{Wind} = CDF_{Waves}$) can be a first approximation if only the distribution of mean wind speeds and significant wave heights is available. The average behavior is met satisfactorily, but in storm conditions, the wave heights are underestimated.

The numerical hindcast puts a high demand on preparation and computational time compared to manual methods. However, it is less costly than long-term measurements and also gives realistic results in which the observed variability in significant wave heights given the mean wind speed is well represented.

The joint distribution model requires synchronously recorded wind and wave data covering larger time histories. If these are available, it is a rather fast approach to set up a realistic model to describe the local wind and wave conditions. The characterization of the single quantities by distribution function not only involves their natural scatter, but also includes information about their mean and mode values as well as about their range of dispersion.

FIGURE 14

Conditional expectation value of the mean wind speed given the significant wave height.

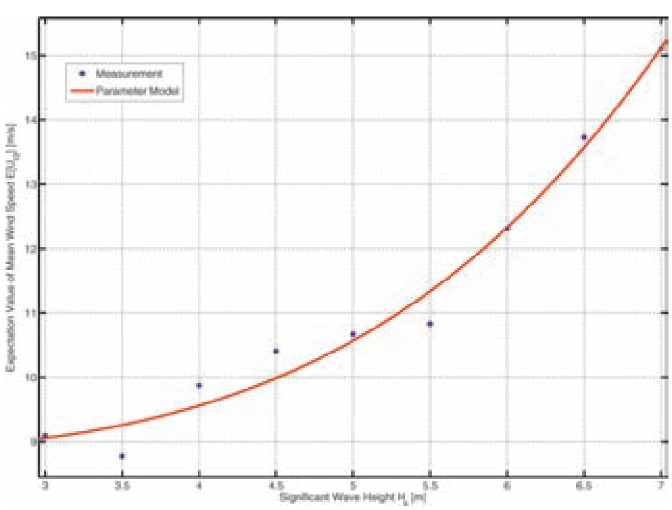

Acknowledgment

The presented work has been funded by the Federal Ministry for the Environment, Nature Conservation and Nuclear Safety of Germany and is part of the research programs GIGAWIND (2000-2003)

and GIGAWIND plus (2004-2007) at the faculty for civil engineering at the University of Hannover. See http://www.gigawind.de for further details on the projects and for publications.

Lead Author:
Kim E. Mittendorf
Vestas Technology R&D
Americas, Inc.
440 Louisiana Street, Ste. 440
Houston, TX 77002
Email: kimit@vestas.com or
kmdorf@aror.de

References

BSH, Bundesamt für Seeschifffahrt und Hydrographie (Federal Maritime and Hydrographic Agency). 2002. Home page. http://www.bsh.de/en/index.jsp (accessed June 2007).

Bouws, E., Günther, H., Vincent., C.L. 1985. Similarity of the wind wave spectrum in finite depth water. J. Geophys. Res. 90 (C1):975-986.

Bretschneider, C. 1952. Revised wave forecasting relationships. In: Proceedings of the 2nd International Conference on Coastal Engineering. Coastal Engineering Research Council of the COPRI (Coasts, Oceans, Ports, Rivers Institute) of the American Society of Civil Engineers. pp. 1-5.

FINO-OFFSHORE. 2004. Research project "FINO – Research Platforms in the North and Baltic Seas". http://www.fino-offshore.com/ (accessed October 2008).

Hasselmann, K., Barnett, T.P., Bouws, E., Carlson, H., Cartwright, D.E., Enke, K., Ewing, J.A., Gienapp, H., Hasselmann, D.E., Kruseman, P., Meerburg, A., Miller, P., Olbers, D.J., Richter, K., Sell, W., Walden, H. 1973. Measurements of wind-wave growth and swell decay during the Joint North Sea Wave Project (JONSWAP) *Ergnzungsheft zur Deutschen Hydrographischen Zeitschrift Reihe*, A(8) (Nr. 12), p. 95.

Meling, T. S., Johannessen, K., Haver, S., Larsen., K. 2000. Mooring analysis of a semi-submersible by use of iform and contour surfaces. In: Proceedings of the OMAE 2000/OSU OFT-4141. The American Society of Mechanical Engineers (ASME International), Ocean, Offshore, and Arctic Engineering (OOAE) Division, New Orleans. pp. 309-316.

Mittendorf, K., Zielke., W. 2004. A hindcast data base for the design of offshore wind energy structures in the German Bight. In: Proceedings of the 29th International Conference on Coastal Engineering. Coastal Engineering Research Council of the COPRI (Coasts, Oceans, Ports, Rivers Institute) of the American Society of Civil Engineers. pp. 740-752.

Mittendorf, K. 2006. Hydromechanical design parameters and design loads for offshore wind energy converters. Dissertation, Institut für Strömungsmechanik, Universität Hannover, Bericht Nr. 71/2006.

Neumann, T., Nolopp, K., Strack, M., Herklotz, K., Stein., J. 2004. Assessment of one year of measurements on the first offshore wind research platform in the German Bight, FINO 1. DEWEK. 1.

Neumann, G, Pierson, W.J. 1966. Principles of Physical Oceanography. Englewood Cliffs, N.J.: Prentice-Hall.

Pierson, W. J., Moskowitz., L. 1964. A proposed spectral form for fully developed wind seas based on the similarity theory of A. A. Kitaigorodskii. J. Geophys. Res. 69: 5181-5190.

Sverdrup, H., Munk., W. 1947. Wind sea, and swell: Theory of relation for forecasting. Technical Report 601. Hydrographic Office, U.S. Navy.

Winterstein, S., Ude, T., Cornell, C., Bjerager, P., Haver, S. 1993. Environmental parameters for extreme response: Inverse form with omission factors. In: Proceedings of ICOSSAR–93, vol. 3. International Conference on Structural Safety and Reliability, International Association for Structural Safety and Reliability.